The Influence of Loading Rate on the Mode III Fracture Properties of Adhesively Bonded Composites

D. PENNAS AND W. J. CANTWELL*
Department of Engineering, University of Liverpool
Liverpool L69 3GH, UK

P. COMPSTON
Department of Engineering, FEIT
Australian National University, Canberra ACT 200, Australia

ABSTRACT: The Mode III interlaminar fracture properties, G_{IIIc}, of an adhesively-bonded glass/epoxy composite are investigated over a wide range of crosshead displacement rates, using the edge crack torsion (ECT) test geometry. The ECT test fixture has been modified to conduct impact testing on these bonded materials. Tests on all of the samples highlighted a significant crack length dependency with the value of G_{IIIc} increasing rapidly with increasing crack length. Tests were also undertaken on the plain glass reinforced epoxy over an equally wide range of crosshead displacement rates.

For a given crack length, the interlaminar fracture toughness of the adhesively-bonded system was superior to that offered by the plain composite, an effect that is attributed to the presence of significant crack-tip blunting within the adhesive layer. The interlaminar fracture toughness of the composite and the adhesively-bonded system remained roughly constant over the range of crosshead displacement rates considered here, suggesting that these systems do not exhibit any significant rate-sensitive fracture behavior. Finally, the crack tip loading conditions are verified by conducting an FEA analysis of the ECT specimen. Here, it was shown that Mode III loading predominates at the center of the test specimen, whereas regions of Mode II loading were observed close to the test supports.

KEY WORDS: delamination, fracture, impact.

INTRODUCTION

FIBER-REINFORCED COMPOSITE MATERIALS offer many advantages over conventional metals such as a high specific strength and stiffness, excellent formability as well as superior long-term fatigue properties. One of the frequently quoted disadvantages of these lightweight materials is their relatively poor resistance to localized impact loading. Extensive experimental testing has shown that even low energy impacts are capable of generating significant internal damage within the structure, which can, in turn, result in a sharp reduction in the residual strength of the structure [1–5].

*Author to whom correspondence should be addressed. E-mail: cantwell@liv.ac.uk
Figure 2 appears in color online: http://jrp.sagepub.com

0731-6844/08/00 0001–14 $10.00/0 DOI: 10.1177/0731684408090716

The examination of failed components has highlighted a number of fracture mechanisms such as fiber cracking, fiber–matrix debonding and delamination. Of these failure processes, delamination is perhaps the most serious, since it can significantly reduce the compressive strength of the composite. Delamination in a structural laminate may consist of the Mode I (opening), Mode II (sliding shear), and Mode III (scissoring shear) components of strain energy release rate. A variety of test techniques including the double cantilever beam (for Mode I loading), the end-notch flexure (for Mode II fracture), and the split cantilever beam (for Mode III loading) have been used in order to characterize the delamination resistance of high performance composite materials [6–11]. These interlaminar fracture tests have shown that the delamination fracture energy of a polymer–matrix composite is generally quite low, with values typically ranging from 100 to 4000 J/m^2. Much of the published work on interlaminar fracture has been undertaken at relatively low rates of loading, typically a few millimetres per minute. However, previous research has shown that many polymeric materials used in the manufacture of composite materials are rate-sensitive and that their fracture toughness properties decrease as the strain rate is increased [12]. One of the earliest attempts to examine the effect of strain rate on the delamination resistance of composites was undertaken by Aliyu and Daniel [13]. Here, the DCB specimen geometry was used in order to study the rate-sensitivity of a carbon–epoxy system. The authors observed a 28% increase in the critical strain energy release rate, G_{Ic}, over approximately three decades of loading rate. Yaniv and Daniel [14] used the height-tapered DCB geometry to achieve higher crack velocities in a carbon fiber reinforced epoxy composite and found that the value of G_{Ic} initially increased with crack velocity up to roughly 1 m/s and then dropped slightly at higher rates.

Work has also been carried out in order to investigate the rate sensitivity of the Mode II interlaminar fracture properties of composites. Maikuma et al. [15] used the center notch flexure specimen to study rate effects in AS4/PEEK. The impact initiation toughness of AS4/PEEK was found to be approximately 20% lower than its static value. Blackman et al. [16] used the end-loaded split test geometry to study rate effects in the Mode II delamination behavior of AS4/PEEK and the carbon fiber/epoxy system T400/6376. No significant dependency of G_{IIc} on loading rate was observed, although a modest reduction was noted at the highest rates of loading.

Little work has been carried out on the Mode III interlaminar fracture properties of composites, mainly because of the difficulties arising from achieving this type of loading [10,17–21]. Donaldson [10] used the split cantilever beam to characterize the Mode III interlaminar fracture properties of a carbon fiber reinforced epoxy composite. Lee [18] subsequently developed the edge crack torsion (ECT) geometry to characterise Mode III failure in composites. This test is based on a laminate that contains a mid-plane delamination which is subjected to torsion. Ratcliffe [20] used the ECT test to characterise the Mode III interlaminar fracture toughness of a carbon fiber and a glass fiber reinforced epoxy resin, where it was shown that the measured values of G_{IIIc} increased rapidly with increasing crack length. The effect of varying fiber volume fraction on the Mode III interlaminar fracture properties of a glass fiber reinforced epoxy laminate was investigated by Li et al. [21], who reported a large increase in Mode III toughness with decreasing fiber volume fraction. They also showed that the measured values of G_{IIIc} varied significantly with crack length in composites with both low and high fiber volume fractions.

The aim of this study is to characterize the rate sensitivity of the Mode III interlaminar fracture properties of an adhesively bonded composite material. With the increasing use of adhesively-bonded structures in a wide range of applications, there is a need to understand

how such systems respond under complex loading conditions at both low and high rates of strain. The data from the tests on the adhesively-bonded structures are then compared with the fracture properties of the plain composite material used in the substrates. A finite element analysis is also used to determine the distribution of the Mode II and Mode III strain energy release rates along the crack front in the adhesively bonded specimens.

EXPERIMENTAL PROCEDURE

The composite used in this research study was a woven glass fiber reinforced epoxy with a fiber volume fraction of 45% (Stesapreg EP127-C15-45 from Stesalit AG). The following stacking sequence was used in the manufacture of the plain composite samples:

$$[90^\circ/0^\circ(+45^\circ/-45^\circ)_2/(-45^\circ/+45^\circ)_20^\circ/90^\circ]\text{s}.$$

During lamination, a folded layer of aluminium foil (0.02 mm thick) was introduced at the laminate mid-thickness to act as a starter defect. Panels with dimensions 200×240 mm were then manufactured in a picture-frame mold using a hot press according to the manufacturer's recommended processing cycle. The nominal final thickness of these glass/epoxy laminates was 6.5 mm. After manufacture, specimens with length 'L' and width 'b' dimensions of 108 and 38 mm respectively were removed from the laminates.

The second part of this study focused on the Mode III fracture properties of an adhesively-bonded GFRP laminate. A two part epoxy resin adhesive (AV138/HV998 from Ciba-Geigy) was used to bond two GFRP laminates based on a stacking sequence of:

$$[90^\circ/0^\circ(+45^\circ/-45^\circ)_2/(-45^\circ/+45^\circ)_20^\circ/90^\circ].$$

The adhesive was cured for 24 h at room temperature. Once again, a folded layer of aluminum foil was introduced at the adhesive mid-thickness to act as a starter defect. The nominal thickness of the adhesively-bonded woven glass/epoxy laminates was 7.9 mm, yielding an approximate thickness of 1.4 mm for the epoxy adhesive. Clearly, this is significantly thicker than a typical adhesive joint and the measured values are likely to be higher than those measured on thinner joints. However, it does enable the Mode III properties of the bulk adhesive to be characterised. After manufacture, specimens with length 'L' and width 'b' dimensions of 108 and 38 mm respectively were removed from the laminates.

The edge crack torsion (ECT) specimen geometry shown in Figure 1 was used to characterise the Mode III interlaminar fracture properties of the plain composite and the adhesively-bonded laminates investigated in this program. The ECT sample is rectangular in shape, with a pre-crack positioned along one edge, as shown in the figure. The distance between the points where the displacement is applied 'l', is equal to 76 mm. Each loading pin is located at a distance of 3 mm in the y-direction from the edge of the specimen.

The test fixture used for loading the ECT samples is shown in Figure 2. Here, the ECT specimen is placed on two supports positioned at diagonally opposite corners of the test sample and the load is applied by two pins located at the two remaining corners. Cylindrical holes machined in the test-frame facilitated the vertical movement of the two loading pins. The precise positioning of the specimen on the ECT fixture was ensured via three guide pins located on two edges of the test sample. Two guide pins are located at the long side of the

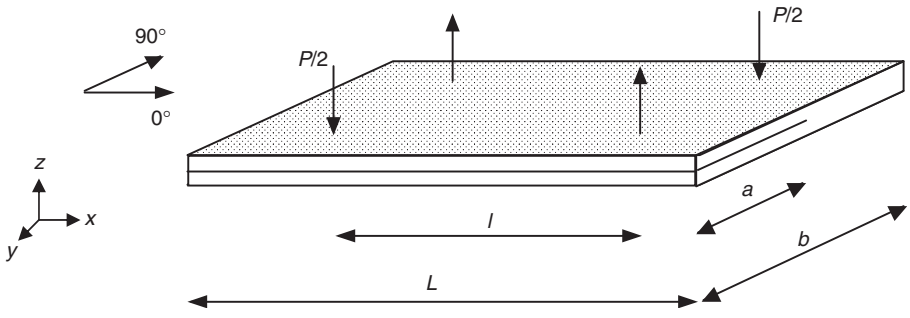

Figure 1. *Schematic of the ECT test specimen.*

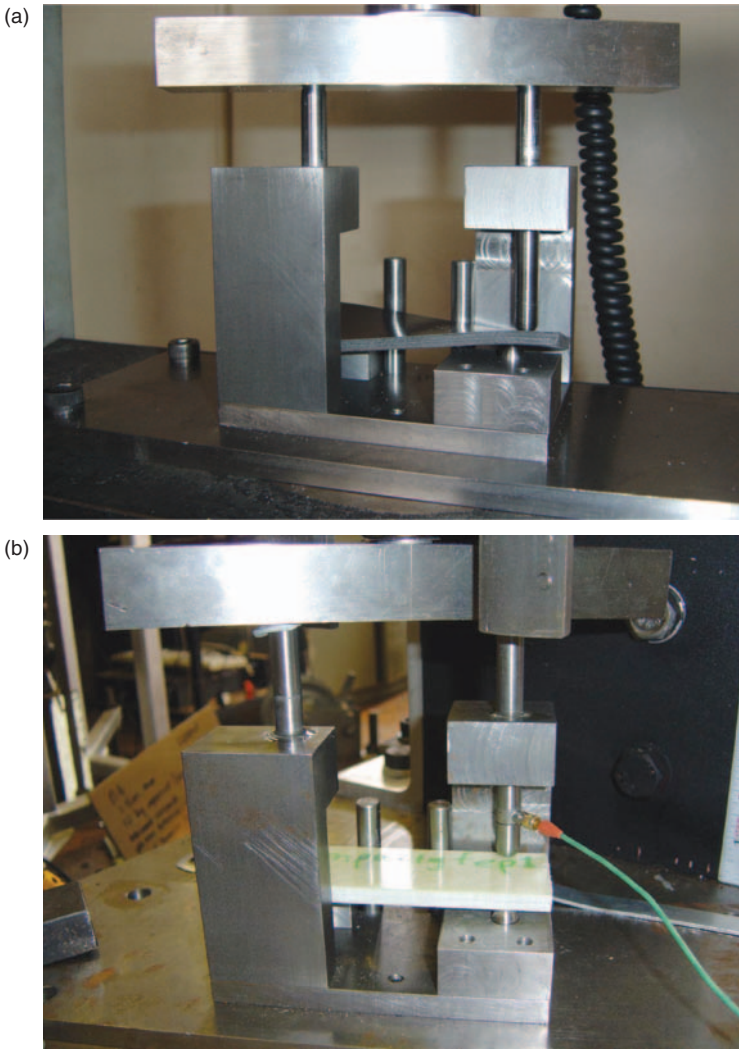

Figure 2. *(a) The ECT test fixture; (b) The modified ECT test fixture for the impact testing.*

specimen at a distance of 40 mm in the x-axis direction from each edge. The third guide pin is located at the middle of the short side of the ECT specimen, as shown in Figure 1. The specimen was loaded by applying a force to a horizontal loading bar placed positioned on top of the two loading pins. Tests on the two types of materials were conducted at crosshead displacement rates of 0.2, 2, 20, and 200 mm/min on an Instron 4505 universal test machine. The specimens were placed on the ECT test fixture, ensuring that contact was made with all three guide pins to ensure precise alignment. Once the specimens had been levelled, load was applied under displacement-control conditions. Data acquisition was assured using a dedicated computer connected to the test machine. Initially, specimens with a normalized crack length, a/b, of 0.5, were tested in order to investigate the rate-sensitivity of the Mode III interlaminar fracture properties. Different normalized insert lengths ranging from 0.2 to 0.7 were used when conducting dynamic tests on the adhesively-bonded woven glass fiber/epoxy material. These tests were undertaken in order to investigate if any crack length effects observed under quasi-static loading were also in evidence at dynamic rates.

Impact tests on the ECT samples were undertaken using an instrumented drop-weight impact tower. In these tests, a piezo-electric load-cell was positioned in one of the two vertical loading pins. The horizontal loading bar was attached to the falling carriage to strike the two vertical loading pins. Prior to testing, a small amount of viscoelastic material was placed on top of the loading pins to cushion the impact of the horizontal loading bar. The total mass of the falling carriage, including the horizontal loading bar, was varied between 3 and 4 kg, depending on the required impact energy. The voltage from the piezo-electric load-cell was recorded on a dedicated computer using the Dataflow software package.

A Cambridge S360 scanning electron microscope was used to examine the Mode III fracture surface morphology. Sections were taken from the center of the test specimens and examined within 2 mm of the starter crack tip. The specimens were coated with a thin layer of gold prior to examination.

DATA REDUCTION TECHNIQUES

A compliance calibration method [20] was used to determine the Mode III toughness properties of the two material systems investigated in this study. Initial attention focused on determining the fracture properties at a crosshead displacement rate of 2 mm/min. Here, the inverse of the specimen compliance, $1/C$, was measured from the initial linear portion of the load–displacement plot. The inverse compliance for each specimen was then plotted as a function of normalized crack length. A straight line was then applied to the data using a linear regression analysis, according to:

$$\frac{1}{C} = A\left[1 - m\left(\frac{a}{b}\right)\right] \tag{1}$$

where the parameters A and m can be determined from the intercept and slope of the graph.

The Mode III fracture toughness of each ECT specimen was calculated from the maximum load on the load–displacement trace, $P_c^{\max}$, using:

$$G_{\mathrm{III}c}(\max) = \frac{mC}{2lb[1 - m(a/b)]}(P_c^{\max})^2. \tag{2}$$

FINITE ELEMENT ANALYSIS

Three-dimensional finite element models of the adhesively bonded woven glass fiber reinforced epoxy ECT specimens were constructed using the ANSYS finite element analysis software package. It should be noted that the epoxy resin used to bond the specimens was modeled as a linear isotropic material. The elastic properties used to model the adhesive and the composite are shown in Table 1.

A fine mesh was used in the vicinity of the delamination front, to accommodate for the rapid change in strain field in this region. When modeling the adhesively-bonded woven glass/epoxy specimens, the element thickness at the delamination front (in the z-axis) was set equal to half the thickness of the epoxy adhesive, since the crack was assumed to be located at the mid-thickness of the adhesive. For purposes of symmetry, the top and bottom plies of the ECT specimen were modeled using a finer mesh with an element size equal to one ply thickness.

Finally, contact elements were used along the delamination plane to prevent mesh interpenetration during the analysis. Relative sliding between points within the delamination region was assumed to be frictionless in nature. The nodes positioned at the location of the guide pins were constrained from moving in the x- and y-axes, thereby maintaining contact between the specimen and the pins throughout the analysis. The support pins were modeled by constraining the contact nodes in the z-axis. A prescribed vertical displacement of 2 mm was applied to the nodes positioned at the load pins and a geometrical nonlinear solution was used in order to update the deformed geometry during the solution process.

The reaction loads at the nodes to which displacements were prescribed were determined and the specimen compliance was calculated by dividing the prescribed displacement by the applied load.

VIRTUAL CRACK CLOSURE TECHNIQUE

The virtual-crack-closure-technique (VCCT) was used to calculate the Mode I, Mode II and Mode III strain energy release rate components along the delamination front for each of the models examined [22]. The VCCT procedure uses the forces along the crack front and the relative displacements of the crack faces behind the crack tip in order to determine the three G components [22]. The strain energy release rate components can be calculated from the work required to close the crack to its original length. For three-dimensional, eight-noded solid elements like the ones used in the current analysis, the values of G_{I}, G_{II}, and G_{III} were calculated using:

$$G_{\mathrm{I}} = \frac{1}{2\Delta A} Z_{Li}(w_{Ll} - w_{Ll^*}) \tag{3}$$

Table 1. Properties of the adhesive and composite used in the FE model.

Woven glass fiber/epoxy		
$E_1 = 25$ GPa	$E_2 = 25$ GPa	$E_3 = 1.75$ GPa
$\nu_{12} = 0.3$	$\nu_{13} = 0.3$	$\nu_{23} = 0.38$
$G_{12} = 3.5$ GPa	$G_{13} = 3.5$ GPa	$G_{23} = 3.25$ GPa
Epoxy resin		
$E = 3$ GPa	$v = 0.3$	

$$G_{\mathrm{II}} = \frac{1}{2\Delta A} Y_{Li}(v_{Ll} - v_{Ll^*}) \tag{4}$$

$$G_{\mathrm{III}} = \frac{1}{2\Delta A} X_{Li}(u_{Ll} - u_{Ll^*}). \tag{5}$$

Here, ΔA is the virtual area and is equal to $\Delta a.B$, in which Δa is the length of the element at the delamination front and B is the width of the element. X_{Li}, Y_{Li}, $Z_{Li\ a}$ are the forces in the x, y, and z axes respectively at the delamination front and u_{L^*}, v_{L^*}, w_{L^*} are the corresponding displacements behind the delamination front. The components of strain energy release rate were then plotted as a function of the position along the delamination front. By summing all of the individual strain energy release rate components,

$$G_T = G_{\mathrm{I}} + G_{\mathrm{II}} + G_{\mathrm{III}} \tag{6}$$

the total strain energy release rate at any location along the delamination front was determined.

RESULTS AND DISCUSSION

Finite Element Model Verification

The accuracy of the finite element procedure was evaluated by comparing the predicted specimen compliances with those determined experimentally from the ECT tests. Figure 3 shows the variation of the inverse of specimen compliance with normalized insert length, a/b, for the adhesively-bonded woven glass fiber reinforced composite. The points in the figure correspond to the experimental data and the solid line represents the predictions of the finite element analysis. From the figure, it is evident that the FE predictions are in reasonably good agreement for both short and long crack lengths; however, there is some discrepancy at intermediate lengths with the experimental data dropping below what is virtually a linear trend in the FE data. The constant 'm' in Equation (1) was calculated from both the predictions of the finite element analysis as well as the experimental data,

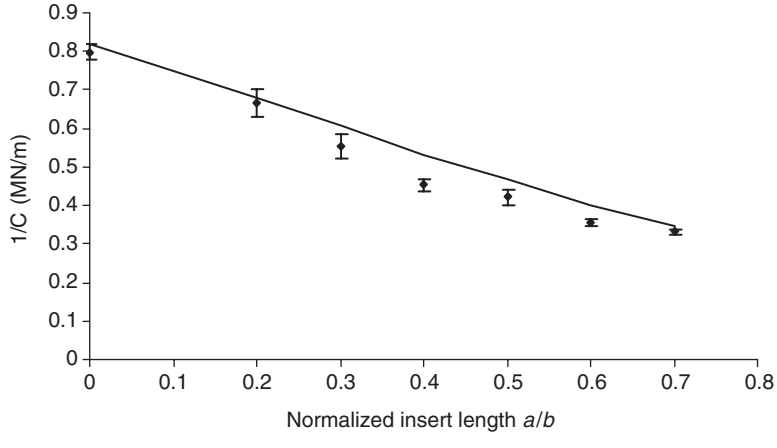

Figure 3. *The variation of the inverse of the specimen compliance with a/b.*

Table 2. Measured and predicted values for the constant m in Equation (1).

	m (experimental)	*m* (FEA)
Woven glass fiber–epoxy	0.73	0.79
Adhesively-bonded composite	0.94	0.87

and the results are presented in Table 2. An examination of this table indicates that the finite element analysis predicts the experimentally–determined values of '*m*' with some success. Similar load-displacement traces were observed following Mode III tests on the plain composite.

Mechanical Testing

Typical examples of experimental load–displacement traces from tests on the adhesively–bonded composites are shown in Figure 4. The load–displacement responses of all of specimens are clearly similar. Typically, the load–displacement plots exhibited a linear response up to the peak force, followed by a sudden drop in load, associated with the crack propagating in an unstable manner along the mid-plane of the sample.

Figure 5 presents plots of the variation of the inverse of specimen compliance with crosshead displacement rate for the adhesively-bonded specimens. The normalized insert length, a/b, was 0.5, for all of the samples shown in the figure. It is evident that specimen stiffness remains constant with crosshead displacement rate. This lack of rate-insensitivity reflects the lack of any rate-depency in the glass fiber composite, since the behavior of this material is likely to dominate the response of these specimens. Unfortunately, the specimen compliance could not be determined at impact rates of strain, since it was not possible to measure the specimen displacement under impact conditions. For the subsequent calculation of the Mode III interlaminar fracture toughness properties, the quasi-static values of '*C*' and '*m*' were used to calculate the Mode III toughness.

Strain Energy Release Rate Distribution

Figures 6 and 7 show plots of the variation of G_{III} and G_{II} along the delamination front for the adhesively-bonded glass fiber reinforced epoxy composites. The Mode II and Mode III strain energy release rates were plotted for normalized insert lengths ranging from 0.2 to 0.7. The Mode I component of the strain energy release rate was found to be negligible relative to the values of G_{II} and G_{III} for all the specimens considered in this study. The Mode II component, G_{II}, was found to peak at positions corresponding to the location of the load and support pins. According to Ratcliffe [20], this is due to the fact that the load and support pins produce a moment arm which causes relative sliding of the two delaminated sections of the specimen, parallel to the direction in which the delamination tends to grow. As a result, G_{II} peaks at the location of the load pins. The previously-stated finding that G_I is very small in these specimens is supported by the fact that relative opening of the delaminated sections of the specimen was also negligible. From the plots of G_{III}, it can be seen that the values of the Mode III strain energy release rate are significantly greater than the corresponding Mode II values. As a result, Mode III is the dominant mode of loading. The predicted distributions for G_{III} suggest that

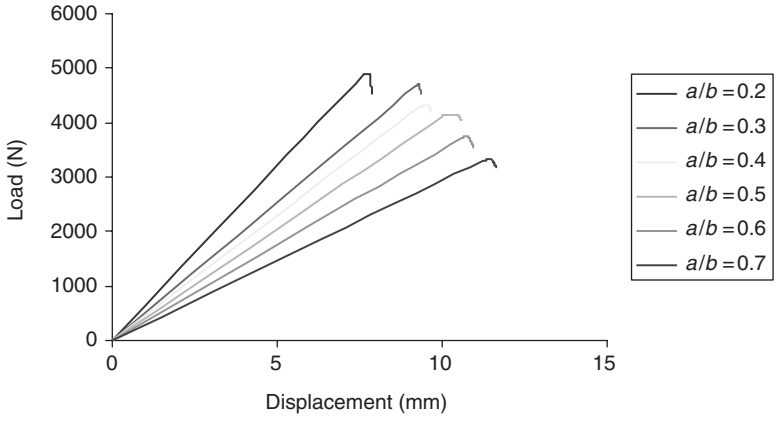

Figure 4. *Load–displacement traces following the ECT tests on adhesively bonded woven glass fiber/epoxy specimens.*

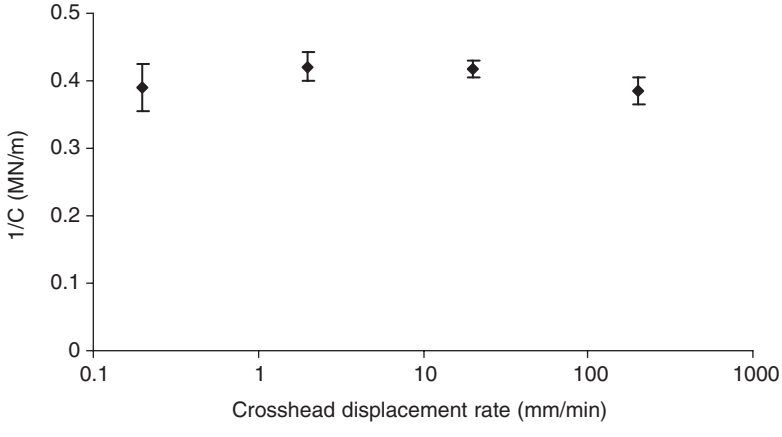

Figure 5. *The influence of crosshead displacement rate on the inverse of specimen compliance for the adhesively-bonded woven glass fiber/epoxy specimens.*

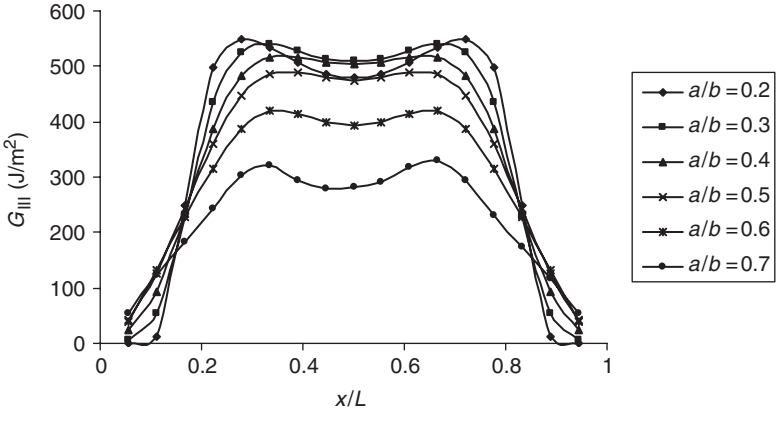

Figure 6. *Mode III strain energy distribution for the adhesively-bonded woven glass fiber/epoxy material as a function of position along the crack front.*

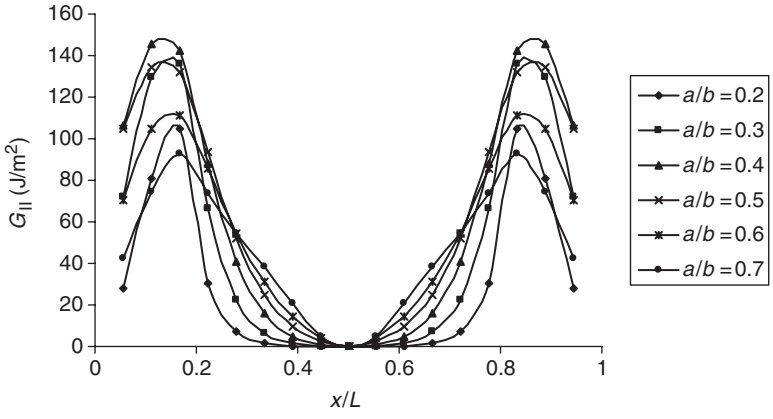

Figure 7. *Mode II strain energy distribution for the adhesively-bonded woven glass fiber/epoxy as a function of position along the crack front.*

delamination should initiate from the central region of the specimen, where the strain energy distribution, G_{III}, is the highest. The finite element predictions indicated that the distributions of G_{II} and G_{III} are similar in the glass/epoxy composite. Similar trends in G_{II} and G_{III} have been observed by other workers following tests on high performance composite materials [20].

Critical Mode III Strain Energy Release Rate of Specimens

The Mode III fracture toughnesses of the adhesively-bonded woven glass fiber/epoxy specimens ECT specimen were calculated using the maximum load in the force–displacement trace, P_c^{max} and Equation (2). Figures 8 and 9 show the critical Mode III strain energy release rate values as a function of the normalized insert length, a/b, for tests performed at a crosshead displacement rate of 2 mm/min and under impact conditions (4.2 m/s), respectively. The Mode III fracture toughness clearly increases with normalized insert length at both loading rates. The values of G_{IIIc} for a given crack length were also very similar at both loading rates. A similar crack length dependency was observed in the plain glass/epoxy composite. It should be noted that the interlaminar fracture toughness of the adhesively-bonded system was found to be significantly higher than that offered by the plain composite. This effect is attributed to the presence of significant crack-tip blunting within the adhesive epoxy layer. Clearly, such blunting will reduce the stress concentrating effect of the pre-crack, leading to an increase in the measured value of toughness.

Figures 10 and 11 show the variation of the Mode III fracture toughness of the two materials as a function of crosshead displacement rate. It should be noted that all of the specimens tested at different crosshead displacement rates were based on a normalized insert length of 0.5. An examination of the data for the plain composite and its adhesively-bonded counterpart indicates that the value of G_{IIIc} remains roughly constant for the crosshead displacements rates examined. The findings suggest that the value of G_{IIIc} (max) appears to be constant with increasing crosshead displacement rate. Blackman and co-workers [16] conducted Mode II fracture toughness tests on a carbon fiber reinforced epoxy composite and showed that G_{IIc} remains roughly constant over a wide range of loading rates. The data for the adhesively-bonded system are very high relative to the plain

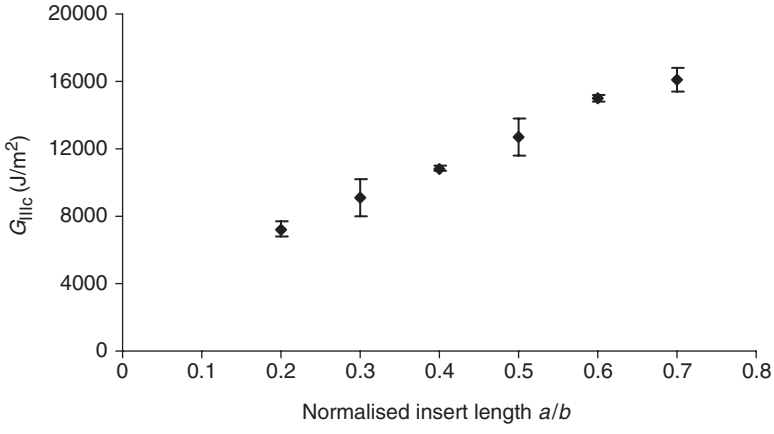

Figure 8. *Mode III critical strain energy release rate versus insert length for the adhesively-bonded woven glass fiber/epoxy specimens tested at a crosshead displacement rate of 2 mm/min.*

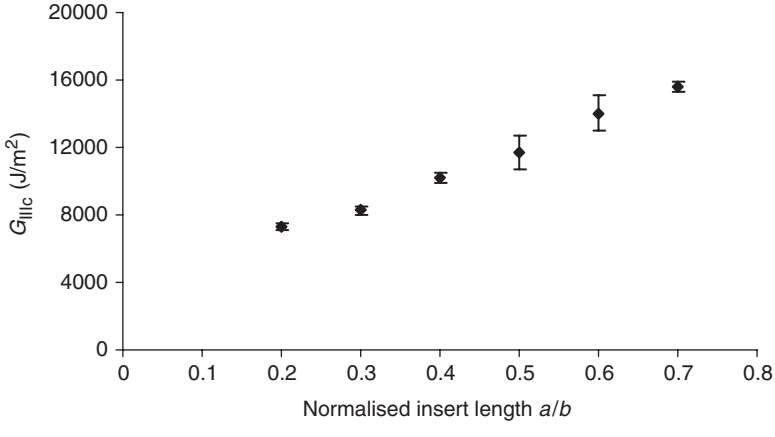

Figure 9. *Mode III critical strain energy release rate versus insert length of adhesively-bonded woven glass fiber/epoxy specimens loaded at 4.2 m/s.*

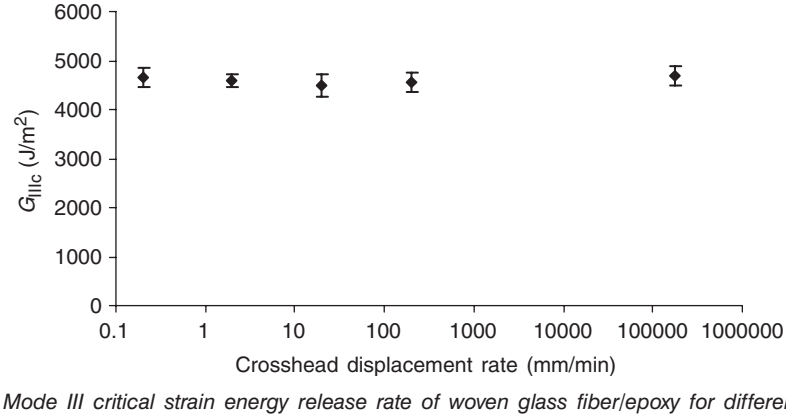

Figure 10. *Mode III critical strain energy release rate of woven glass fiber/epoxy for different crosshead displacement rates.*

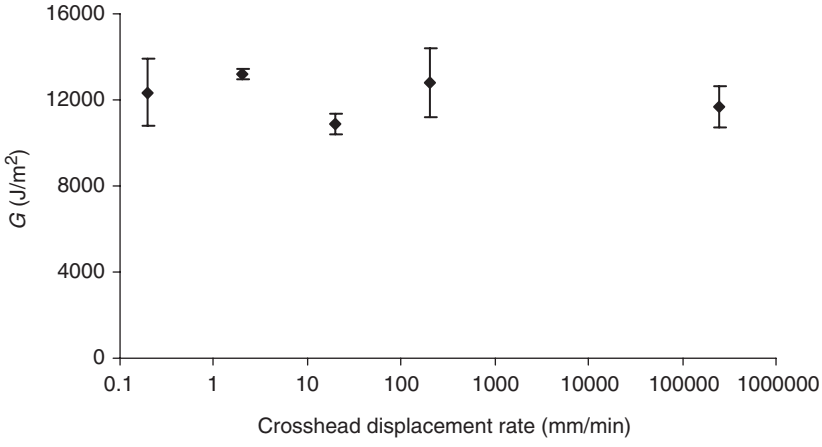

Figure 11. *The variation of Mode III critical strain energy release rate with crosshead displacement rate for the adhesively-bonded woven glass fiber/epoxy.*

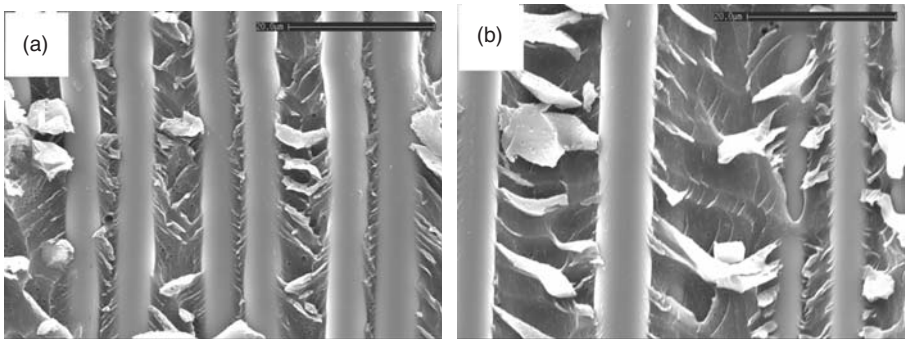

Figure 12. *Fracture surface micrographs of plain composite samples tested at (a) 20 and (b) 200 mm/min.*

composite, the reason for this being partly due to the significant crack-length dependency apparent in Figures 8 and 9. Clearly, if a smaller value of a/b had been selected for these tests at higher rates, then lower values of G_{IIIc} would be apparent in Figure 11. The data in Figure 11 do, however, highlight the rate-insensitivity of the Mode III fracture toughness of the adhesive. An examination of the data indicates that there is greater scatter in the bonded composite than in the plain composite, which may be due to variations in the thickness of the bond line and variability in the degree of adhesion along the adhesive-composite interface.

Fracture surface electron micrographs for the plain composite tested at 20 and 200 mm/min are shown in Figure 12. There is hackle mark deformation in the matrix, which is a significant energy absorbing mechanism under Mode II loading. However, in Mode II the hackle markings are usually perpendicular to the fiber orientation, whereas in this case, Mode III, the hackle markings are oriented at an angle to the fibers (up to 45°). This is particularly evident in Figure 12(a). The hackle mark features were similar in samples for each loading rate, supporting the conclusion from the G_{IIIc} results that there is no effect of loading rate.

Fracture surface examination of the adhesively bonded composite samples revealed features that provide an explanation for the higher G_{IIc} results for this composite.

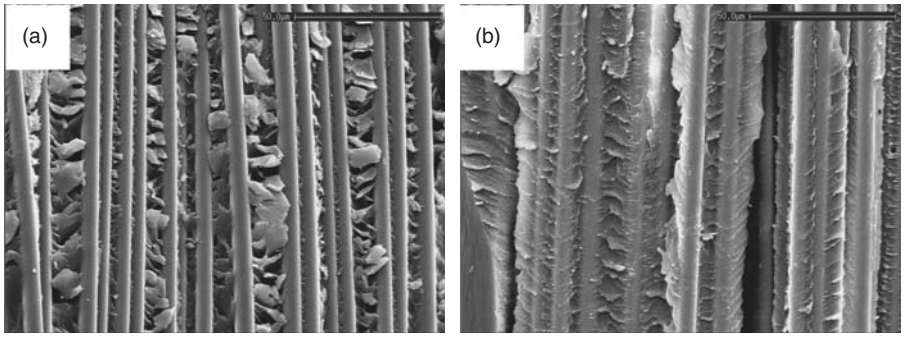

Figure 13. *Fracture surface micrographs of adhesively bonded composite samples tested at (a) 20 and (b) 200 mm/min.*

Again, the micrographs from samples tested at 20 and 200 mm/min, Figure 13, represent the typical features observed at all rates of testing. The surface of the sample tested at 20 mm/min in Figure 13(a) shows hackle marks in the resin matrix, similar to the hackle marks seen in the plain composite, and clean fibers indicate significant interfacial failure. As noted already, these failure modes are major energy absorbing mechanisms. The surface of the sample tested at 200 mm/min in Figure 13(b) shows fibers still covered in the epoxy adhesive, indicating failure through the adhesive layer that was used to bond the composite. The surfaces of all adhesively-bonded composite samples showed evidence of both failure modes seen in Figures 13(a) and (b), indicating that crack propagation deviated between the composite-adhesive interface, and through the adhesive. This tortuous crack path would result in greater energy absorption for the adhesively-bonded composite.

CONCLUSIONS

An investigation has been carried out to investigate the Mode III interlaminar fracture properties of an adhesively-bonded woven glass fiber reinforced epoxy and its plain composite counterpart. A finite element analysis of the edge crack torsion specimens has shown that a region of pure Mode III shear exists at the center of the specimen, whereas zones of locally-high Mode II components of the strain energy release rate exist near the locations of the load and support pins. The experimental data shows that the Mode III interlaminar fracture toughness increases with crack length for both the adhesively-bonded system and the plain composite. A finite element analysis was performed on the adhesively-bonded woven glass fiber reinforced epoxy composite and the findings of this analysis support the experimental data. Rate effects in the Mode III fracture properties of the bonded system and the plain composite were investigated by conducting tests at crosshead displacement rates up to 3 m/s, where, it was shown that the Mode III interlaminar fracture toughness of the plain composite and the adhesively-bonded system remained constant for crosshead displacement rates ranging from 0.2 mm/min up to the impact conditions. The values of the Mode III fracture toughness of the adhesively-bonded woven glass fiber reinforced epoxy were found to be greater than those of the plain composite, probably due to crack tip blunting.

ACKNOWLEDGMENTS

The authors are grateful to the EPSRC for financing part of this study. The microscopy work was undertaken in the Electron Microscope Unit at the Australian National University.

REFERENCES

1. Schoeppner, G. A. and Abrate, S. (2000). Delamination Threshold Loads for Low Velocity Impact on Composite Laminates, *Composites Part A – Applied Science and Manufacturing*, **31**: 903–915.
2. Prichard, J. C. and Hogg, P. J. (1990). The Role of Impact Damage in Postimpact Compression Testing, *Composites*, **21**: 503–511.
3. Cantwell, W. J. and Morton, J. (1989). Comparison of the Low and High-velocity Impact Response of CFRP, *Composites*, **20**: 545–551.
4. Dorey, G., Bishop, S. M. and Curtis, P. T. (1985). On the Impact Response of Carbon Fibre Laminates with Epoxy and PEEK Matrices, *Composites Science and Technology*, **23**: 221–237.
5. Dear, J. P. and Brown, S. A. (2003). Impact Damage Processes in Reinforced Polymeric Materials, *Composites Part A – Applied Science and Manufacturing*, **34**: 411–420.
6. Stevanovic, D., Kalyanasundaram, S., Lowe, A. and Jar, P. Y. B. (2003). Mode I and Mode II Delamination Properties of Glass/vinyl-ester Composite Toughened by Particulate Modified Interlayers, *Composites Science and Technology*, **63**: 1949–1964.
7. Hiley, M. J. (2000). Delamination between Multi-directional Ply Interfaces in Carbon-epoxy Composites under Static and Fatigue Loading, in Fracture of Polymers, Composites and Adhesives, In: Williams, J. G. and Pavan, A. (eds), ESIS Publication, Vol. 27, pp. 61–72.
8. Jordan, W. M., Bradley, W. L. and Moulton, R. J. (1989). Relating Resin Mechanical Properties to Composite Delamination Fracture Toughness, *Journal of Composite Materials*, **23**: 923–943.
9. Pereira, A. B., de Morais, A. B., de Moura, M. F. S. F. and Magalhaes, A. G. (2005). Mode I Interlaminar Fracture of Woven Glass/epoxy Multidirectional Laminates, *Composites Part A – Applied Science and Manufacturing*, **36**: 1119–1127.
10. Donaldson, S. L. (1988). Mode III Interlaminar Fracture Characterization of Composite Materials, *Composites Science and Technology*, **32**: 225–249.
11. Meziere, Y., Michel, L. and Carronnier, D. (2000). Mixed-mode Delamination Failure in Carbon Fiber/Composites under Quasi-static and Cyclic Loading, Fracture of Polymers, Composites and Adhesives, In: Williams, J. G. and Pavan, A. (eds), ESIS Publication, Vol. 27, pp. 97–110.
12. Grein, C., Kausch, H. H. and Beguelin, P. (2003). Characterisation of Toughened Polymers by LEFM using an Experimental Determination of the Plastic Zone Correction, *Polymer Testing*, **22**: 733–746.
13. Aliyu, A. A. and Daniel, I. (1985). *Delamination and Debonding of Materials*, In: Johnson, W. S. (ed.), ASTM STP876, p. 336.
14. Yaniv, G. and Daniel, I. M. (1988). *Height-tapered Double Cantilever Beam for Study of Rate Effects on Fracture Toughness of Composites*, ASTM STP972, pp. 241–258.
15. Maikuma, H., Gillespie, J. W. and Wilkins, D. J. (1990). Mode II Interlaminar Fracture of the Center Notch Flexural Specimen under Impact Loading, *Journal of Composite Materials*, **24**: 124–149.
16. Blackman, B. R. K., Dear, J. P., Kinloch, A. J., MacGillivray, H., Wang, Y., Williams, J. G. and Yayla, P. (1996). The Failure of Fibre Composites and Adhesively Bonded Fibre Composites under High Rates of Test – Mixed Mode I/II and Mode II Loadings, *Journal of Materials Science*, **31**: 4467–4477.
17. Cantwell, W. J. (1998). The Interlaminar Fracture Properties of Composite Materials at High Rates of Strain, *Key Engineering Materials*, **141–143**: 463–476.
18. Lee, S. M. (1993). An Edge Crack Torsion Method for Mode III Delamination Fracture Testing, *Journal of Composites Technology and Research*, **15**: 193–201.
19. Li, J., Lee, S. M., Lee, E. W. and O'Bien, T. K. (1997). Evaluation of the Edge Crack Torsion (ECT) Test for Mode III Interlaminar Fracture Toughness of Laminated Composites, *Journal of Composites Technology and Research*, **19**: 174–183.
20. Ratcliffe, J. G. (2004). Characterization of the Edge Crack Torsion (ECT) Test for Mode III Fracture Toughness Measurement of Laminated Composites, NASA/TM-2004-213269.
21. Li, X., Carlsson, L. A. and Davies, P. (2004). Influence of Fiber Volume Fraction on Mode III Interlaminar Fracture Toughness of Glass/Epoxy Composites, *Composites Science and Technology*, **64**: 1279–1286.
22. Shivakumar, K. N., Tan, P. W. and Newman, J. C. (1988). A Virtual Crack Closure Technique for Calculating Stress Intensity Factors for Cracked Three-dimensional Bodies, *International Journal of Fracture*, **36**: R43–R50.